Journal of Polymer Research (2021) 28: 114
https://doi.org/10.1007/s10965-021-02471-8

ORIGINAL PAPER

Preparation, characterization, and performance of bio-based polyester composites derived from renewable distillers grains and shellfish

Chin-San Wu[1] · **Dung-Yi Wu**[2] · **Shan-Shue Wang**[1]

Received: 31 December 2020 / Accepted: 25 February 2021/ Published online: 13 March 2021

Abstract

Although biocomposites typically display poor performance, this deficiency can be mitigated by incorporating suitable bio-fillers with the base biopolymer. The main objective of this study was to assess the effectiveness of distillers grains and *Paphia undulata* shell mixture when used as fillers to improve the functional performance of polylactic acid (PLA). The MPLA/TTDGP (modified polylactic acid, MPLA; coupling agent-treated distillers grains powder, TDGP; and *P. undulata* shell powder heat-treated at 900 °C, TPUSP) and PLA/DGP (polylactic acid/distillers grains powder) composites were prepared via a melting and mixing process, and then their structural, thermal, mechanical and anti-oxidant properties, as well as their biocompatibility and biodegradability, were characterised. Compared with MPLA and PLA, the tensile properties were obviously enhanced in the MPLA/TTDGP and PLA/DGP composites. The tensile strength at failure (δ) and Young's modulus (E) of MPLA/TTDGP were approximately 5–37 and 50–1,200 MPa higher, respectively, than those of PLA/DGP, due to better interfacial adhesion. The water resistance values of the MPLA/TTDGP and PLA/DGP composites were also increased compared with MPLA and PLA. The water resistance was greater in the MPLA/TTDGP composite than the PLA/DGP composite. Both PLA/DGP and MPLA/TTDGP composites displayed good biocompatibility. DGP increased the polyphenol content, and enhanced the antioxidant properties and biodegradability, of the PLA/DGP and MPLA/TTDGP composites, while TPUSP enhanced the antibacterial properties of the MPLA/TTDGP composite.

Keywords Antibacterial properties · Biodegradability · Distillers grains powder · *Paphia undulata* shell powder · Polylactic acid · Tensile properties

Introduction

The development of environmentally friendly materials is of increasing interest because widespread discarding of petrochemical polymers [1–3] leads to environmental pollution and ecological damage. Globally, petrochemical-based polymer products are being replaced increasingly by bio-based polymers and their composites [4–10]. Among current bio-based polymers, polylactic acid (PLA) [11], polybutylene succinate adipate [12] and polybutylene adipate-co-terephthalate [13] are the most accepted, with PLA being a key biodegradable polymer.

PLA can be produced by ring-opening polymerisation of cornstarch. It has good mechanical properties, processability, biocompatibility, and biodegradability [14, 15], and it is suitable for packaging materials, biomedical materials, and daily necessities [16, 17]. Although PLA is relatively expensive, it can be mixed with waste resources from catering services, such as distillers grains and shell powder, to reduce costs and enhance their mechanical properties and functional development [18, 19].

The catering drink industry, in which beer accounts for a large proportion, continues to grow, and the distillers grain waste that remains after the brewing process is increasing accordingly. At present, most of this waste is treated by incineration and composting, which pollutes the environment and wastes natural resources [20]. The main component of distillers grain waste is wheat plant fibre, which is characterised by their biodegradability, biocompatibility, low cost, and low density [21, 22]. As distillers grain waste contains large amounts of cellulose, lignin, and

✉ Chin-San Wu
t50008@cc.kyu.edu.tw; cws1222@cc.kyu.edu.tw

[1] Department of Applied Cosmetology, Kao Yuan University, Kaohsiung City 82101, Taiwan, Republic of China

[2] Department of Materials Science and Engineering, Johns Hopkins University, Baltimore, MD 21218, USA

other hemicelluloses, it represents a macromolecular filling material with good reinforcement effects that can effectively reduce the cost of composites. Moreover, because distillers grain waste is a renewable catering material, it will be increasingly used in the future [23]. Many researchers have studied composites based on distillers grain waste and polymers. Tisserat et al. [24] ground spent distillers grains, oil, and fat and removed polar extracts using an organic solvent. The remaining high fibre content mixture was modified with a coupling agent and mixed with plastics to create a composite. The spent distillers grains show a good reinforcement effect and tend to enhance the tensile strength and flexural property of composites. Li et al. [25] dried distillers grains in a vacuum. After crushing, alkaline treatment and a silane coupling agent treatment, the residue was blended with a polymer to create a composite; in this composite, the interfacial compatibility between the polymer and distillers grains was enhanced, as were the tensile strength and elongation at break [25]. Although waste distillers grains can reinforce the properties of polymers, the addition of antibacterial supplements to improve the functional characteristics of these composites requires further development.

The increasing consumption of shellfish by the catering and food processing industries is increasing the amount of generated waste, which is leading to additional environmental pollution. Various approaches have been explored to solve this issue. For example, $CaCO_3$, which is the main component of shells, can be transformed by different processes into CaO or $Ca(OH)_2$, which are promising as antibiotic polymer additives. Hadiyanto et al. [26] cleaned *Paphia undulata* shells, ground them into a 100-μm fine powder, and then calcined them at 800 °C for 3 h, thereby converting the $CaCO_3$ into CaO. Kao et al. [27] calcined waste freshwater shells to obtain CaO at 800 °C, which was blended with polyethylene to form a composite that could be used as blown-film food packaging. The packaging material was antibacterial and prolonged the shelf life of food. These studies demonstrate that shellfish waste (e.g. oyster shells, scallop shells, and *P. undulata* shells) can be processed at high temperatures to obtain natural additives having antibiotic activity.

In this study, two types of treated food waste were combined with polymers to form low-cost functional composites. The waste materials were pre-processed, and the PLA was modified to improve the interfacial properties of ternary-blend composites. Part I of this paper details the removal of impurities from the distillery residue waste and treatment of the remaining powder with a silane coupling agent to obtain treated distillery residue powder. Part II describes the high-temperature calcination of the powder at 900 °C, whereupon the $CaCO_3$ in the *P. undulata* shell is converted into $Ca(OH)_2$ and CaO. Part III describes the modification of PLA by acrylic acid (AA) to increase the compatibility between PLA and the two waste materials and thereby enhance interfacial adhesion. The structural features, oxidation resistance, mechanical strength, antibacterial properties, biocompatibility, and biodegradability of the ternary blend composites are discussed here, from the perspective of future applications in food-packaging films, cosmetics, stationery, and biomedical engineering packaging materials.

Experimental section

Materials

The PLA (Purapol L130) was provided by Corbion Co., Ltd. (Amsterdam, The Netherlands). Tetraethoxysilane (TEOS) was purchased from Merck Chemical Co. (Frankfurt, Germany). Gallic acid monohydrate, AA, dimethyl sulphoxide (DMSO), 2,2-diphenyl-1-picrylhydrazyl (DPPH), dicumyl peroxide (DCP), Folin–Ciocalteu phenol reagent, and sodium carbonate (anhydrous) (Na_2CO_3) were obtained from Sigma-Aldrich Corp. (St. Louis, MO, USA). Promega Corp. (Madison, WI, USA) supplied the 3-(4,5-dimethylthiazol-2-yl)-2,5-diphenyltetrazolelium bromide (MTT). Dulbecco's modified Eagle's medium (DMEM) and foetal bovine serum (FBS) were purchased from Gibco-BRL (Gaithersburg, MD, USA). Measurement of the AA loading quantity for dichloromethane (DCM)-soluble PLA was performed by titration; the grafting percentage was 5.92 wt% [28]. The DCP and AA loadings were maintained at 0.3 and 10 wt%, respectively. All buffers and other reagents were of high-purity commercial grade.

Treatment and fabrication of distillers grains and *P. undulata* shell powder

Distillers grain (DG) was obtained from Taipei Brewery (Taiwan). The DG was made up of a mixture of fine orange pieces (length: 3–5 mm). The crude DG was dried *in vacuo* at 50–60 °C for 2 days. The grain was abraded in a high-speed rotary grinder (Yowlin Industrial Co. Ltd., Taiwan) and then dried in vacuum. The crushed DG was then filtered through 500-mesh (25-μm) and subsequently 625-mesh (20-μm) sieves to obtain distillers grains powder (DGP).

DGP treated with coupling agents (TDGP) was prepared as follows. DGP (10 g), 1 g of silane coupling agent, and acetone were mixed in a beaker for 18 h. The mixture was maintained at room temperature for 10 h after sealing the bottle neck with a membrane. Then, the sample was rinsed with acetone and dried in an oven at 80 °C for 1 day. The DGP processing steps are illustrated in Scheme 1.

Paphia undulata shell (PUS) was acquired from Xingda Fishing Port in Kaohsiung (Taiwan). The PUS was cleaned with water to remove surface dirt and impurities, dried in a

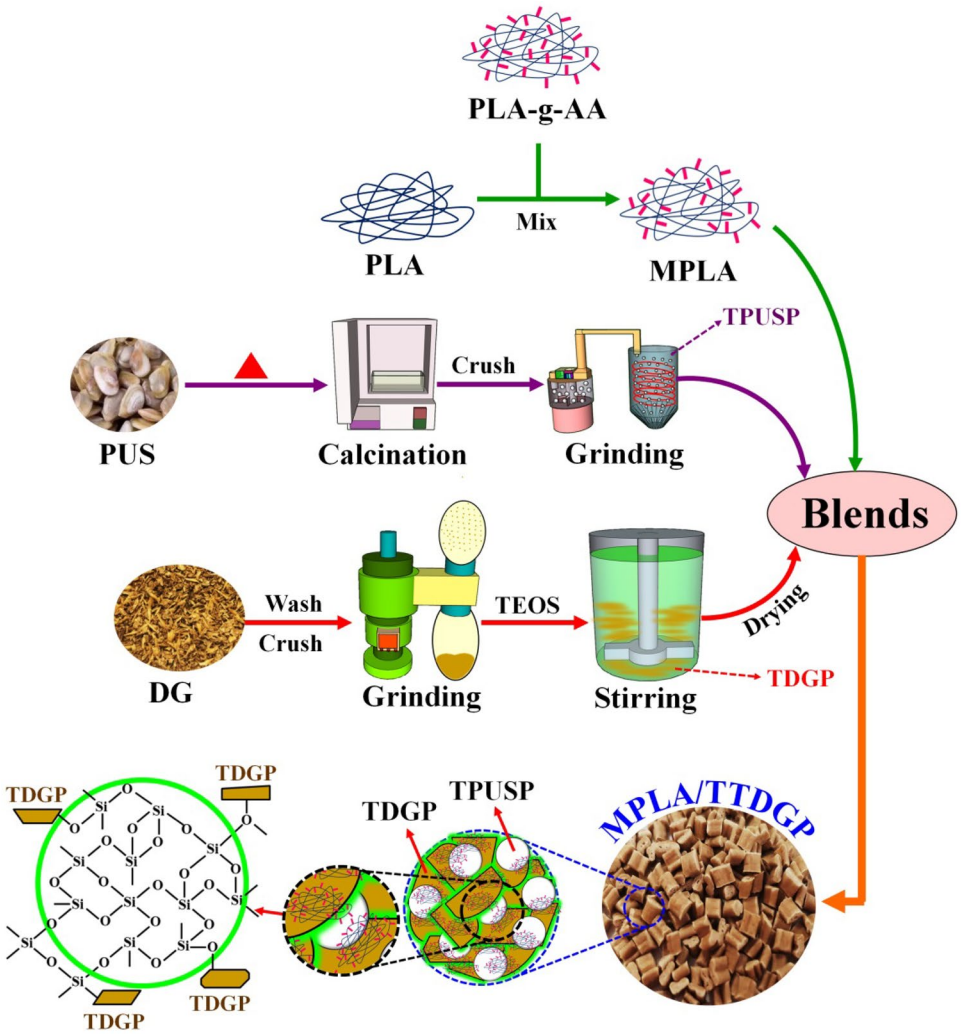

Scheme 1. Schematic diagram of the fabrication of MPLA/TTDGP composites containing modified polylactic acid (MPLA), treated (coupling agent) distillers grains powder (TDGP) and thermally treated *Paphia undulata* shell powder (TPUSP)

vacuum oven at 100–110 °C for 1 day, ground and sieved through 800–2,500 mesh screens to obtain a 5–15-μm fraction of *P. undulata* shell powder (PUSP), and thermally treated at 900 °C for 3 h in a calcinatory. The calcined PUSP was then cooled to room temperature to obtain thermally treated PUSP (TPUSP). The overall TPUSP processing step is described in Scheme 1.

Processing of the composites

The DGP or TTDGP samples were rinsed with acetone and then dried in an oven at 105 °C for 18 h. The blends were mixed at a rotor speed of 50 rpm in a Brabender Plastograph W50EHT 200-Nm mixer with a blade-type rotor (Brabender Instruments, Inc., Hackensack, NJ, USA) at 170–180 °C for 20 min. The composites were then cast into thin plates with a hot press, cooled in a dryer, and finally cut to the appropriate size for further study. Scheme 1 shows the entire process for fabricating a new ternary composite composed of MPLA, TPUSP, and TDGP. Table 1 summarises the components of all samples included in this study.

Characterisation

The samples were analysed by Fourier transform-infrared (FT-IR) spectroscopy [28], wide-angle X-ray diffraction (XRD) [29], tensile testing [28], differential scanning calorimetry (DSC) [30], and scanning electron microscopy (SEM) [31], according to the cited references.

Contact angles were determined using a contact angle meter (model 100SB; Sindatek Instruments Co., Ltd., New Taipei, Taiwan). Samples were mounted on a platform after drying in an oven at 60 °C. Deionised water (DI, 2 μL) was dropped for sampling and the contact angle was measured and recorded.

Water absorption [32] was measured according to the standard ASTM D570. Specimens had the dimensions of $30 \times 20 \times 0.5$ mm^3. All specimens were dried and weighed. Then, the samples were immersed in water for 1 day.

Table 1 Formulation of PLA/DGP and MPLA/TTDGP composites

Sample code	Component			
	PLA (wt%)	PLA-g-AA (phr)	DGP/TDGP (wt%)	TPUSP (phr)
PLA	100	-	-	-
PLA/DGP 10wt%	90	-	10	-
PLA/DGP 20wt%	80	-	20	-
PLA/DGP 30wt%	70	-	30	-
PLA/DGP 40wt%	60	-	40	-
MPLA	100	10	-	-
MPLA/TTDGP10wt%	90	10	10	5
MPLA/TTDGP 20wt%	80	10	20	5
MPLA/TTDGP 30wt%	70	10	30	5
MPLA/TTDGP 40wt%	60	10	40	5

PLA polylactic acid, *MPLA* modified PLA *DGP* distillers grains powder, *TDGP* coupling agent treated distillers grains powder, *TPUSP Papia undulata* shell powder heat treated at 900 C, *TTDGP* TDGP and TPUSP mixed complex

Next, the water droplets on the sample surface were gently removed with a tissue. The water absorption (m_w) was estimated as follows:

$$\%m_w = \frac{m_1 - m_0}{m_0} \times 100\% \quad (1)$$

where m_0 is the dried sample weight before testing and m_1 is the treated sample weight after eliminating excess water.

Polyphenols content assay

The total phenolic content was measured according to the Folin–Ciocalteu method [33]. A sample (0.001 g) of DGP, PLA/DGP, or PLA/TTDGP was dispersed in 20 mL of DCM solution (1:1 v/v DCM:water). A mixture containing 0.2 mL of each solution, 1 mL of 50% Folin–Ciocalteu reagent, 0.2 mL of methanol, and 1 mL of water was incubated in a 35 °C water bath for 5 min. Then, a 0.02 mL of 5% Na_2CO_3 was added to the solution, and the solution was stored in the dark for 1 h. The solutions were then assessed at 725 nm using a spectrophotometer. The tests were repeated three times, and the average polyphenol content was calculated.

Antioxidant assay

The antioxidant activity of the composites was measured according to the DPPH method [34]. Samples (0.002 g) of DGP, PLA/DGP, and PLA/TTDGP composites were separately dissolved in 10 mL of chloroform. An aliquot (0.8 mL) was removed and blended with DPPH solution (0.2 mL). The mixture was then kept in the dark for 1 h. The absorbance was determined at 515 nm. The DPPH radical-scavenging activity (%RSA) was calculated as follows:

$$\%RSA = \left(1 - \frac{A_C - A_S}{A_c}\right) \times 100 \quad (2)$$

where A_S and A_C represent the sample and control absorbances, respectively. The values are the averages of three replicates.

In vitro cytotoxicity test

All of the composites were sterilised with 70% alcohol, followed by ultraviolet light exposure for 30 min. Cell viability was analysed using an MTT assay according to our previous study [35]. The sample film was cultured with normal human foreskin fibroblasts (WS-1, BCRC60300) at 37 °C for 3 days. Subsequently, the cells were continuously cultured for 1, 3, and 5 days after replacing with fresh medium. MTT (100 µL) was added to each 24-well plate, and the plates were incubated for 5 h. Then, 150 µL of DMSO was added after removing the supernatant. The absorbance was measured at 540 nm using a PowerWave XS reader (Bio-Tek Instruments Inc., Winooski, VT, USA). The average is reported for five replicated specimens.

Antibacterial activity

The bacterial inhibition of PLA/DGP and MPLA/TTDGP composites was tested against *Escherichia coli* (BCRC10239) and *Staphylococcus aureus* (BCRC10780T) bacteria [29]. Chips (1 g) of PLA/DGP and MPLA/TTDGP were incubated in 25 mL of culture medium with 5×10^6 cells at 37 °C for 18 h. The bacterial inhibition was then determined.

Biodegradation test

The degradation of PLA, MPLA, and their composites in the soil experiment was assessed according to the method of Wu et al. [31]. The $35 \times 20 \times 0.5$ mm^3 rectangular composite specimens were prepared and buried in a soil container at a humidity of 40–50% at 25–30 °C. Specimens of the buried PLA, MPLA, and their composites were removed every 10 days, cleaned with water, and then dried at 50 °C. The percentage of weight loss was determined as the average of at least six measurements. Surface changes of the specimens were examined by SEM.

Statistical analysis

All of the experiments were replicated three times ($n = 3$). Data were analysed by one-way analysis of variance and

t-tests. The data are presented as the mean ± standard error. *P*-values < 0.05 were considered to be statistically significant.

Results and discussion

Structural analyses of PLA and their composites

Figure 1 presents the FT-IR spectra of DGP, silane coupling agent, and TDGP. The wide absorption peak at 3,503 cm^{-1} for DGP was shifted to 3,492 cm^{-1} for TDGP (Fig. 1). This shift is attributable to less hydrogen bonding in TDGP compared to DGP, as the free –OH groups in DGP were reduced in TDGP when DGP converted to TDGP [36]. The absorption peaks at 1,086 and 808 cm^{-1} in silane are associated with the asymmetric stretching of Si–O–C and/or Si–O–Si bonds [37]. Therefore, the TDGP spectra indicate polysiloxane deposition on the DGP.

Figures 2a, b present the main regions of the FT-IR spectra corresponding to PLA and MPLA. Figure 2b shows the 1,711 cm^{-1} spectra of the AA group in MPLA; similar results have been reported previously [28].

Figures 2c, d present the characteristic absorption ranges of the PLA/DGP and MPLA/TTDGP composites, respectively. The peak at 3,200–3,600 cm^{-1} attributable to O–H stretching behaviour intensified in PLA/DGP (Fig. 2c); the single extra peak at 3,301 cm^{-1} was attributed to the –OH group of DGP. For PLA/DGP and MPLA/TTDGP, the vibration band broadened and shifted from 3,301 to 3,274 cm^{-1}, respectively (Figs. 2c, d). All observations showed strong hydrogen bonding between the carboxylic groups of the MPLA matrix and the Si–OH groups of TDGP. The four new peaks at 579, 811, 873, and 1,733 cm^{-1} (Fig. 2d) are associated with the reaction between AA in MPLA and –OH in TDGP and TPUSP. These peaks were attributed to the asymmetric stretching behaviours of Si–O–Si and CaO bonds and the ester stretching vibration of MPLA/TTDGP, respectively [29, 30]. Taken together, these results demonstrate the enhanced interfacial adhesion of MPLA, TDGP, and TPUSP, compared with DGP and MPLA.

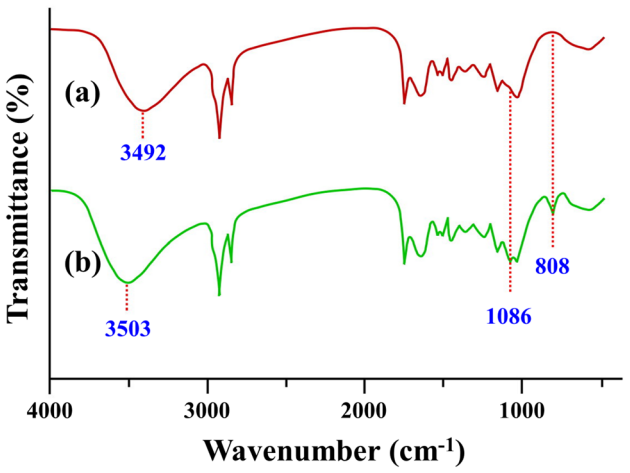

Fig. 1 Fourier transform-infrared spectra of (**a**) distillers grains powder (DGP) and (**b**) coupling agent-treated DGP (TDGP)

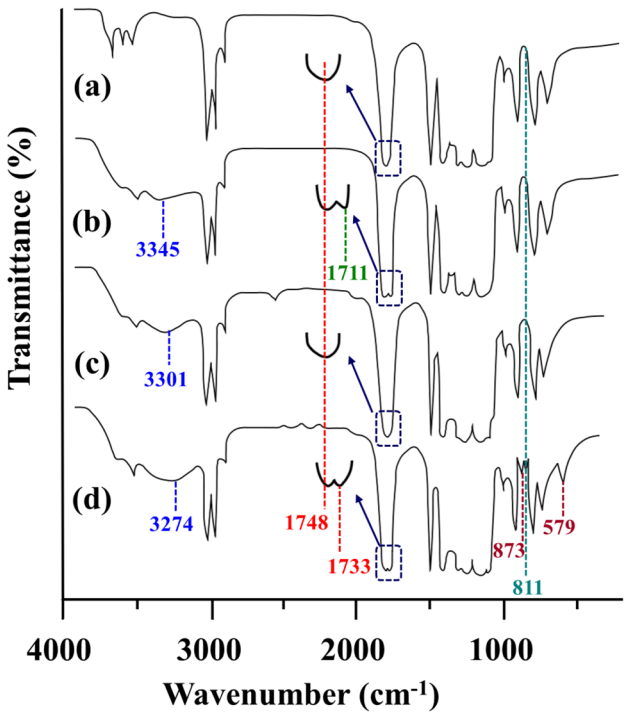

Fig. 2 Fourier transform-infrared spectra of (**a**) polylactic acid (PLA), (**b**) modified PLA (MPLA), (**c**) PLA/DGP (20 wt%) and (**d**) MPLA/TTDGP (20 wt%). TTDGP: TDGP and TPUSP (or *P. undulata* shell powder heat-treated at 900 °C)

The crystallisation properties of pristine PLA, PLA/DGP (20 wt%), and MPLA/TTDGP (20 wt%) were also evaluated using XRD (Fig. 3). Similar to the results reported by Wu and Tsou [38], pristine PLA exhibited two peaks at 16.9° and 19.6° (Fig. 3a). Compared with pristine PLA (Fig. 3a), two extra peaks appeared at about 15.2° and 21.9° in the XRD spectrum of PLA/DGP composites (Fig. 3b), mainly contributed by DGP (Fig. 3d) [39]. These peaks showed that DGP was well-distributed in the PLA matrix. Three new peaks at 18.2°, 29.3° and 34.3° emerged in the XRD spectra of MPLA/TTDGP composites (Fig. 3c), compared with those of PLA/DGP composites (Fig. 3b). The peaks at 29.3° and 34.3° are features of TPUSP. Wu [40] illustrated that the peak at 18.2° is due to ester bond formation, reflecting the structural differences between PLA/DGP and MPLA/TTDGP.

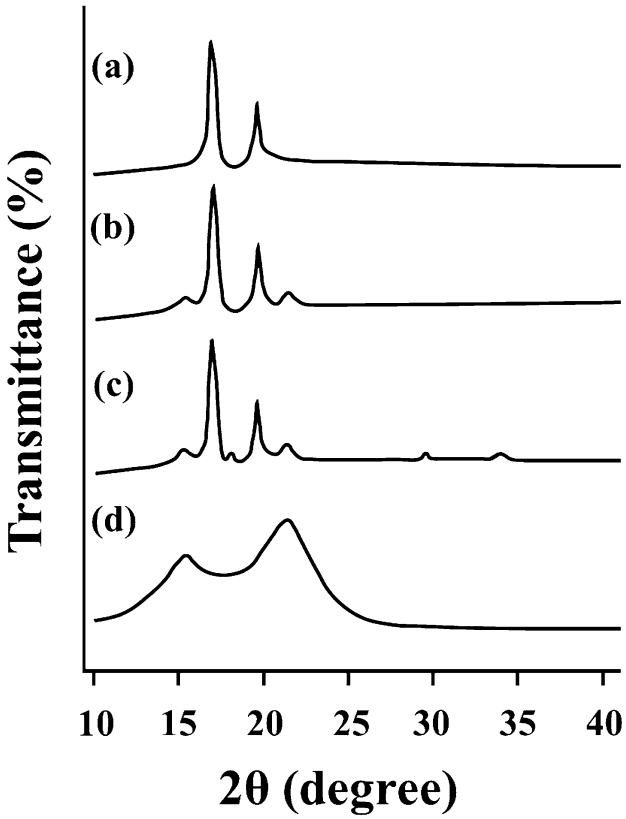

Fig. 3 Wide-angle X-ray diffraction patterns of (**a**) PLA, (**b**) PLA/DGP, (**c**) MPLA/TTDGP and (**d**) DGP

Thermal properties of PLA and their composites

Table 2 summarises data from DSC heating thermograms on the melting enthalpy (ΔH_m), glass transition temperature (T_g), and melting temperature (T_m) of PLA/DGP and MPLA/TTDGP composites containing varying amounts of DGP or TTDGP. T_m increased with decreasing DGP or TTDGP content for both composites; this was most likely due to a loose polymer structure resulting from PLA or MPLA expansion caused by DGP or TTDGP. The MPLA/TTDGP composite had a lower T_m than the PLA/DGP composite. T_g increased with DGP or TTDGP content for both composites. The reduced space for molecular motion is reasonably explained by this phenomenon [41]. The 5–8 °C T_g was higher for the MPLA composite, as the modification of AA onto PLA further limited molecular motion.

The ΔH_m of MPLA (36.3 J g^{-1}) was lower than that of PLA (36.9 J g^{-1}). There were more grafted branches in MPLA, which destroyed the PLA structure and increased the space between chains, thus resulting in a lower ΔH_m value. The ΔH_m values ranged from 6–11 J g^{-1} for MPLA/TTDGP composites, and were higher than in PLA/DGP analogues due to the condensation reaction. The crystallinity was well correlated with ΔH_m. The DGP or TTDGP increase was associated with a decrease in ΔH_m in both the PLA/DGP and MPLA/TTDGP composites (Table 2). However, a significant decrease in ΔH_m was observed for PLA/DGP, indicating a lower degree of crystallinity [42].

Phase morphology and mechanical properties of PLA and their composites

The surface morphology of composites was examined by SEM (Fig. 4). Poor cohesion was observed between the DGP and the PLA matrix in PLA/DGP (20 wt%) (Fig. 4a). TTDGP and the MPLA matrix showed improved adhesion in MPLA/TTDGP (20 wt%) (Fig. 4b) due to the bond between them. Table S3 lists the tensile strengths at failure (δ), and the Young's modulus (E) for the PLA/DGP (20 wt%) and MPLA/TTDGP (20 wt%) composites as a function of DGP or TTDGP content. δ and E of pristine PLA (43.2 ± 1.0/3,560 ± 35 MPa) decreased after conversion to MPLA (41.8 ± 1.3/3,503 ± 37 MPa). Additionally, δ and E decreased significantly with increasing DGP content (from 43.2 ± 1.0/3,560 ± 35 to 23.3 ± 2.3/2,920 ± 52 MPa) for the PLA/DGP composites (Table 3). Thus, these results are an indication of the poor adhesion of DGP in the PLA matrix, as shown in Fig. 4a. The MPLA/TTDGP composites (Table 3) showed unique behaviour with respect to δ and E; specifically, δ and E increased with TTDGP content up to 20 wt%, despite MPLA having a lower δ and E than pristine PLA. Above 20 wt% TTDGP content, these values decreased sharply; this decrease was attributed to aggregation of the TTDGP. Additionally, the δ and E of MPLA/TTDGP were approximately 5–37 and 50–1,200 MPa higher, respectively,

Table 2 Effect of DGP or TTDGP content on the thermal properties of PLA/DGP and MPLA/TTDGP composites

DGP or TTDGP (wt%)	PLA/DGP			MPLA/TTDGP		
	Tg	Tm	ΔH_m	Tg	Tm	ΔH_m
0	57.5	162.1	36.9	57.1	161.5	36.3
10	59.3	160.2	29.1	65.3	156.3	35.1
20	60.6	159.3	26.1	68.3	153.8	33.8
30	61.5	158.6	23.9	69.0	153.5	32.9
40	62.8	158.0	21.7	69.6	153.1	32.5

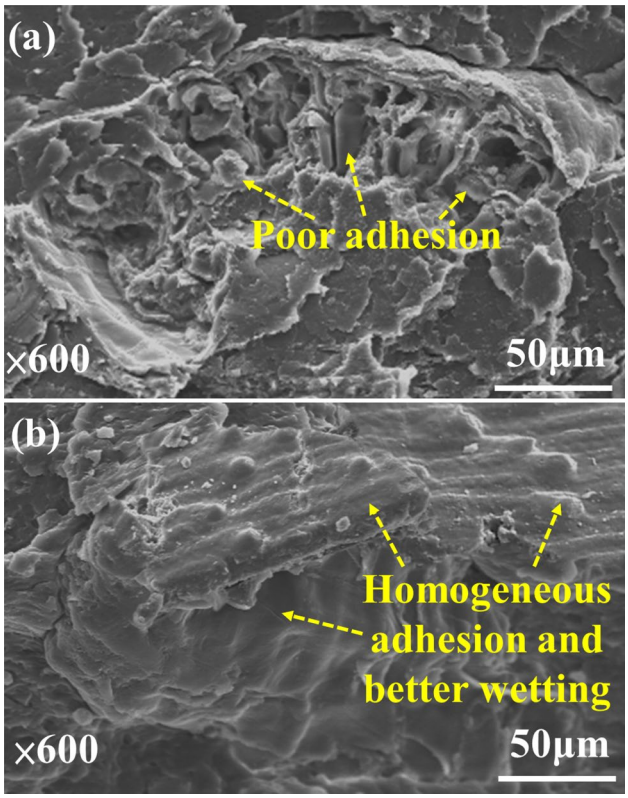

Fig. 4 Scanning electron microscopy images illustrating the adhesion and distribution of fibre powder in the (**a**) PLA/DGP (20 wt%) and (**b**) MPLA/TTDGP (20 wt%) composites

than those of PLA/DGP. The results listed in Table 3 suggest that the MPLA/TTDGP composite improved δ and E of PLA/DGP.

Surface wettability, water absorption, and the biological activity of PLA and their composites

Figure 5 presents the contact angles for PLA, MPLA, and their composites. The values were similar for PLA and MPLA, while that for MPLA was slightly lower than that

Table 3 Effects of DGP/or TTDGP content on the tensile properties of PLA/DGP and MPLA/TTDGP composites. δ: tensile strength at failure and E: Young's modulus

DGP or TTDGP (wt%)	PLA/DGP		MPLA/TTDGP	
	E (MPa)	σ (MPa)	E (MPa)	σ (MPa)
0	3560 ± 35	43.2 ± 1.0	3503 ± 37	41.8 ± 1.3
10	3320 ± 40	38.8 ± 1.5	3890 ± 38	54.3 ± 1.9
20	3206 ± 45	33.6 ± 1.8	4346 ± 40	65.8 ± 2.1
30	3108 ± 48	27.7 ± 2.1	4196 ± 41	62.3 ± 2.3
40	2920 ± 52	23.3 ± 2.3	4021 ± 45	59.8 ± 2.5

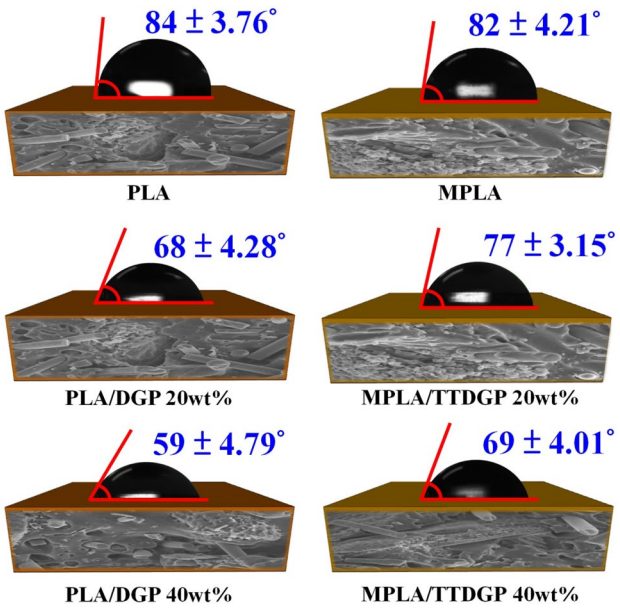

Fig. 5 Contact angles of PLA, MPLA and their composites

for PLA. This reduction was attributed to the –COOH functional groups of MPLA that enhanced the hydrophilicity of the polymer. Pristine PLA had the largest contact angle. DGP is comprised of many –OH groups, which increased the hydrophilicity and reduced the contact angle when DGP was added. However, the contact angle of MPLA/TTDGP was higher than that of PLA/DGP because the esterification partially depleted the hydroxyl groups in TTDGP and the carboxyl groups in MPLA. The formation of ester bonds was verified by FT-IR analysis.

Figure 6a compares the water absorption rate of membranes of the PLA/DGP and MPLA/TTDGP composites after different immersion times. The water absorption rate of both membranes increased with DGP or TTDGP content and immersion time. Water was readily absorbed due to the hydrophilicity of DGP and TTDGP. Additionally, for the same DGP or TTDGP content and immersion time, the MPLA/TTDGP membrane had lower water absorption than the PLA/DGP membrane. This indicates that the MPLA/TTDGP composite was more hydrophobic. The hydrophobicity of TTDGP made water permeation unlikely. Hence, the MPLA/TTDGP displayed better water resistance.

The biocompatibility of PLA, MPLA and their composites was examined by WS-1 FB cell viability. The PLA/DGP and MPLA/TTDGP sample composites were cultured with WS-1 FB cells for 1, 3, and 5 days. Cell growth was not statistically different among the control and treated groups at day 1, and the apparent increases observed at days 3 and 5 were also not statistically different. The cell growth with 40% PLA/DGP and 40%

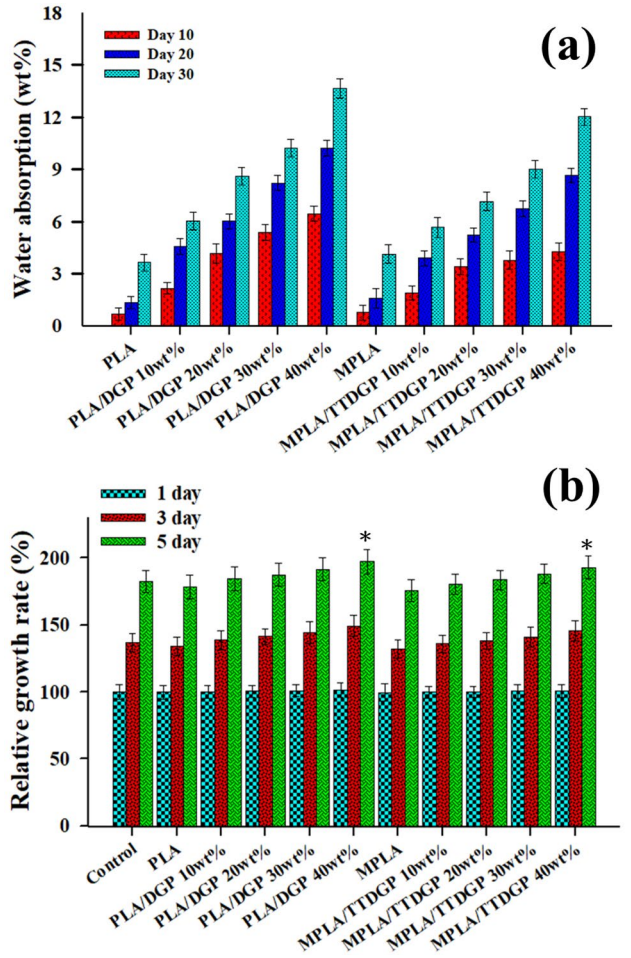

Fig. 6 (**a**) Percent mass gain from the absorption of water for PLA, MPLA and their composites. (**b**) Cell viability of WS-1 cells seeded on PLA, MPLA and their composites. Cell viability was measured quantitively using MTT assay. The data were analysed using *t*-tests, with significant differences (*) determined at the $p < 0.05$ level for each treatment versus the control group

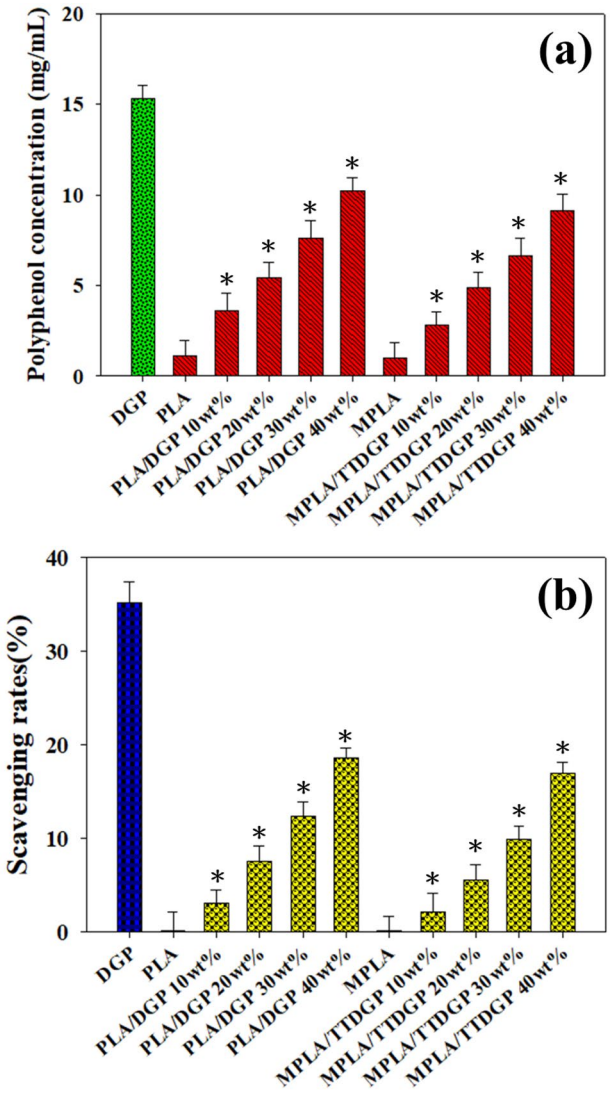

Fig. 7 (**a**) Polyphenols content of PLA, MPLA and its composites. (**b**) DPPH radical-scavenging activity assays of PLA and MPLA and its composites. The data were analysed using *t*-tests, with significant differences (*) at the $p < 0.05$ level for each treatment versus the control group

MPLA/TTDGP became statistically significant on day 5 ($p < 0.05$) (Fig. 6b). These results indicate that the PLA/DGP and MPLA/TTDGP composites had good biocompatibility.

Polyphenols content and antioxidant properties of PLA, MPLA and their composites

Figure 7a presents the polyphenol contents of DGP, PLA/DGP, and MPLA/TTDGP composites. Pristine DGP had the highest polyphenol content at 15.32 mg/mL. Pristine PLA and MPLA composites had the lowest polyphenol content at 1.12 and 0.99 mg/mL, respectively. DGP was the major polyphenol contributor [43]. In the PLA/DGP and MPLA/TTDGP composites, the polyphenol content increased with increasing DGP or TTDGP content. Additionally, the polyphenol content was slightly higher in PLA/DGP composites than MPLA/TTDGP composites. Compared with PLA bonded to DGP, MPLA had more polyphenols bonded to TTDGP, thus reducing the amount of free polyphenols.

Figure 7b presents the antioxidant activities of PLA, MPLA, and their composites. Pristine PLA and MPLA lacked antioxidant activity and thus were the controls. The polyphenols in DGP were also a major source of antioxidant activity [44]. The free-radical scavenging activity reached 35.26% at 0.05 mg/mL of DGP. Moreover, the free-radical scavenging activity of PL/DGP and MPLA/TTDGP increased with DGP and TTDGP content in PL/DGP and

MPLA/TTDGP (Fig. 7b). Essentially, greater DGP content contributed more polyphenols.

Antibacterial activity assay

Figure 8a presents the antibacterial activities of membranes of PLA, MPLA, and their composites against *E. coli* (Gram-negative) and *S. aureus* (Gram-positive). There was no inhibition zone in the PLA-, MPLA- or PLA/DGP-treated areas cultured with either bacteria. However, the MPLA/TTDGP 20 wt% and 40 wt% samples generated inhibition zones of radii 0.42 and 0.44 cm for *E. coli* and 0.33 and 0.34 cm for *S. aureus*, respectively. The antibacterial effect was attributed mainly to CaO in the TPUSP [45]. The inhibition activity of MPLA/TTDGP against *S. aureus* was less than that of *E. coli* due to the stronger cell wall (and thus better protection) of *S. aureus*.

The antibacterial activity of PLA, PLA/DGP, and MPLA/TTDGP membranes were examined quantitatively in a liquid culture containing the bacteria and the membranes. After 18 h of cultivation, PLA and PLA/DGP did not annihilate *E. coli* or *S. aureus*; however, the MPLA/TTDGP membrane significantly inhibited bacterial growth (Figs. 8b and 9). The antibacterial effect was thus attributed to the TPUSP content of the membrane.

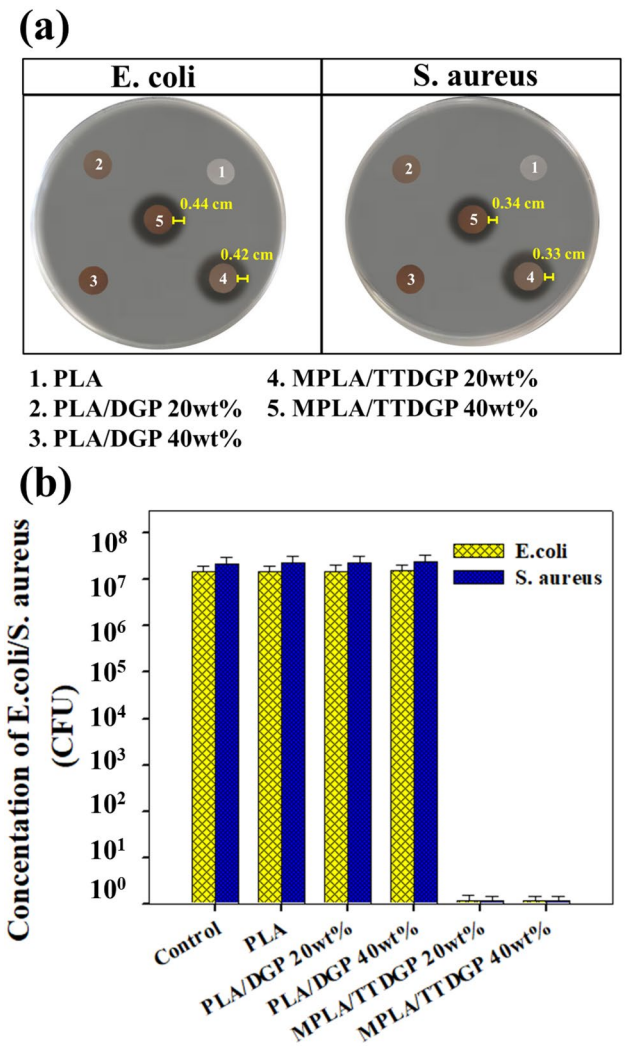

Fig. 8 (**a**) Antibacterial activity of PLA, MPLA and its composites against *Escherichia coli* and *Staphylococcus aureus*. The inhibition zone is equivalent to the radius of the clear zone. (**b**) Viable bacteria were quantitatively measured after the PLA, PLA/DGP and MPLA/TTDGP composites were placed in liquid medium containing *E. coli* or *S. aureus* and cultured for 18 h

Biodegradation of PLA and their composites

Figure 10 presents SEM micrographs of PLA/DGP and MPLA/TTDGP composite surfaces on days 30 and 60 of the soil test. Both PLA/DGP (20 wt%) and MPLA/TTDGP (20 wt%) composites displayed larger and deeper pits than the PLA materials. The MPLA/TTDGP (20 wt%) composite (Figs. 10h, i) had more evenly distributed, smaller pits than PLA/DGP (20 wt%) (Figs. 10e, f). The DGP biodegradation in PLA/DGP (20 wt%) and MPLA/TTDGP (20 wt%) composites increased with increasing time and was obvious at day 60. The MPLA/TTDGP (20 wt%) composite degraded more slowly than PLA/DGP (20 wt%), which is in good agreement with the results presented in Fig. 11. These results show that the addition of DGP to PLA and TTDGP to MPLA enhanced the biodegradability of these composites.

The weight loss of PLA, MPLA, and the PLA/DGP and MPLA/TTDGP composites was measured after various incubation times in soil (Fig. 11). All of the materials showed degradation progression as the incubation time increased. The weight losses observed for the PLA/DGP and MPLA/TTDGP composites were greater than those of PLA and MPLA. Higher DGP and TTDGP contents in PLA/DGP and MPLA/TTDGP specimens, respectively, increased degradation. The 40% DGP and TTDGP contents in PLA/DGP and MPLA/TTDGP specimens had the fastest degradation rates, which increased rapidly over the initial 30 days and then stabilised at 50–60 days. The 5–13% weight loss was higher for PLA/DGP than MPLA/TTDGP, but MPLA/TTDGP degraded more slowly than PLA/DGP (Figs. 10 and 11). The improved resistance to water and microbes generated in the soil was attributed to the strong interfacial bonding of MPLA with TTDGP.

Conclusions

A new type of composite material, MPLA/TTDGP, was prepared and characterised. Re-utilisation of food wastes, such as DGP and PUSP, was the focus of this research. Converting PLA into MPLA improved interfacial compatibility. DGP was

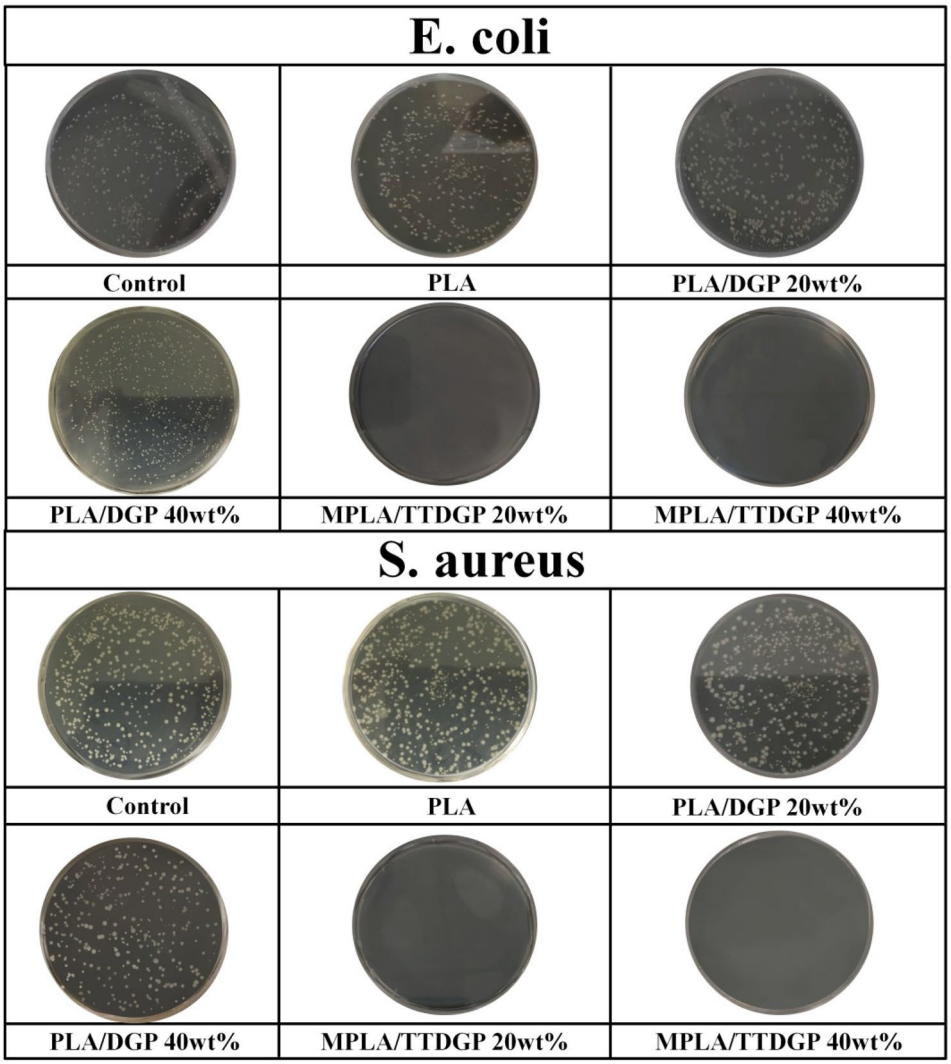

Fig. 9 The number of viable bacteria was determined from photographs of PLA, PLA/DGP, and MPLA/TTDGP composites placed in liquid medium containing *Escherichia coli* or *Staphylococcus aureus* and cultured for 18 h

processed with a coupling agent to form TDGP, and PUSP was converted to TPUSP by heating at 900 °C. An MPLA/TTDGP composite was prepared. The structural, thermal, tensile, antioxidant, antibacterial, biological and biodegradable properties were elucidated. The tensile properties of the MPLA/TTDGP composite were superior to those of PLA/DGP. Various analytical techniques (FT-IR, XRD, and SEM) confirmed the better dispersion of TTDGP in the MPLA matrix compared with DGP in the PLA matrix. Ester bond formation between the –OH groups of TTDGP and the AA groups of MPLA is a rational explanation for the improved dispersion. The MPLA/TTDGP composites displayed uniform distribution with good adhesion between the TTDGP and MPLA matrix, and a greater water contact angle than the corresponding PLA/DGP composite. The PLA/DGP and MPLA/TTDGP composites also displayed good cell viability, as well as antioxidant and antibacterial properties. Biodegradation of MPLA/TTDGP was less than that of PLA/DGP in a soil test, and the degradation rates were higher for MPLA/TTDGP and PLA/DGP than pure PLA and MPLA. Greater DGP and TTDGP content in the composites resulted in a more rapid degradation. These novel MPLA/TTDGP composites can be readily produced at a large scale for many applications, such as packaging films with antibacterial activity and daily necessities such as utensils (e.g. plates, utensils/chopsticks, bowls, and straws) and stationery (e.g. pens, pen boxes, and paper clips).

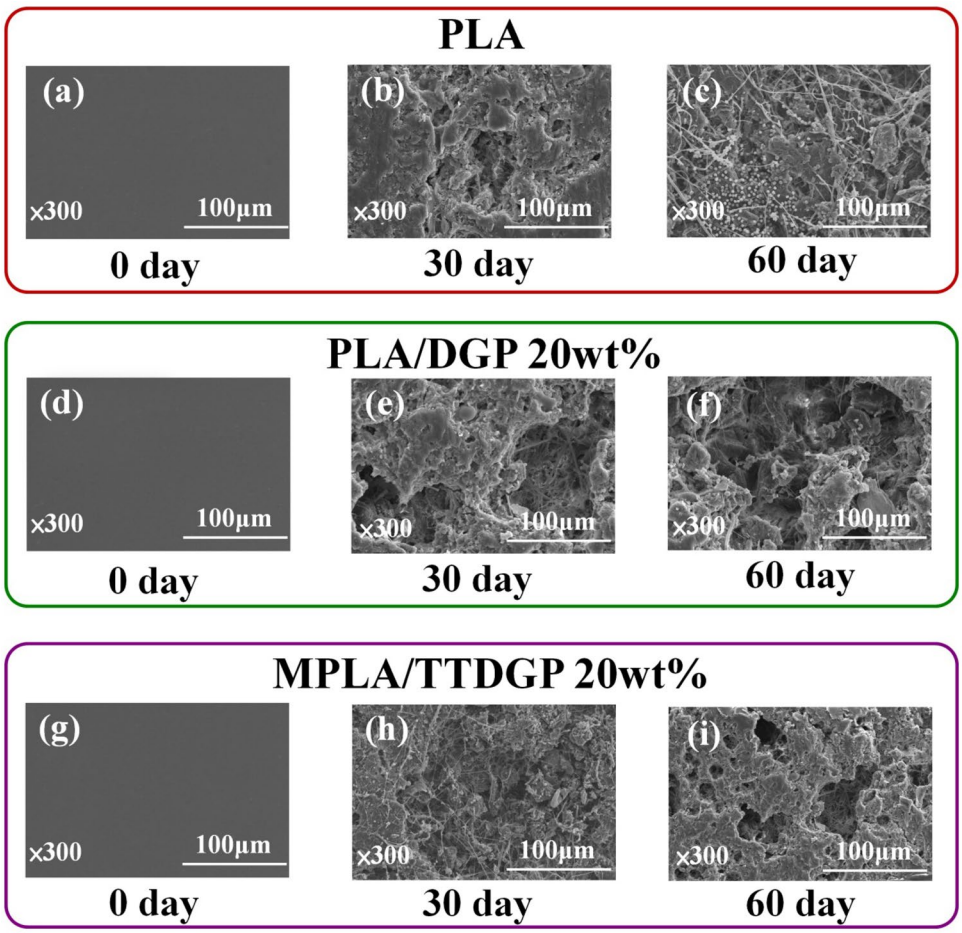

Fig. 10 Scanning electron microscope images illustrating the morphology of (**a–c**) PLA, (**d–f**) PLA/DGP (20 wt%) and (**g–i**) MPLA/TTDGP (20 wt%) composites as a function of incubation time in soil

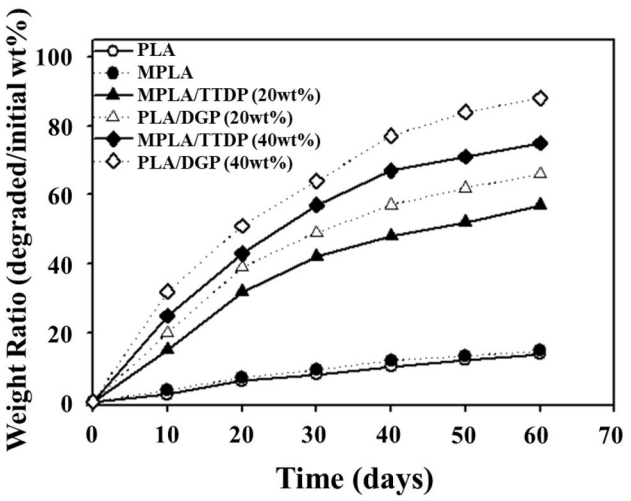

Fig. 11 Weight loss of PLA, MPLA and their composites as a function of the soil incubation period

Acknowledgment The author thanks the Ministry of Science and Technology (Taipei City, Taiwan, R.O.C.) for financial support (MOST-109-2221-E-244-003).

Declarations

Conflict of interest The authors declare no competing financial interest.

References

1. Sharma B, Jain P (2020) Deciphering the advances in bioaugmentation of plastic wastes. J Clean Prod 275:123241. https://doi.org/10.1016/j.jclepro.2020.123241
2. Larrain M, Passel SV, Thomassen G, Kresovic U, Alderweireldt N, Moerman E, Billen P (2020) Economic performance of pyrolysis of mixed plastic waste: Open-loop versus closed-loop recycling. J Clean Prod 270:122442. https://doi.org/10.1016/j.jclepro.2020.122442
3. Valerio O, Muthuraj R, Codou A (2020) Strategies for polymer to polymer recycling from waste: Current trends and opportunities for improving the circular economy of polymers in South America. Curr Opin Green Sustain Chem 25:100381. https://doi.org/10.1016/j.cogsc.2020.100381

4. Wang Z, Ganewatta MS, Tang C (2020) Sustainable polymers from biomass: Bridging chemistry with materials and processing. Prog Polym Sci 101:101197. https://doi.org/10.1016/j.progpolymsci.2019.101197
5. Dubey SP, Thakur VK, Krishnaswamy S, Abhyankar HA, Marchante V, Brighton JL (2017) Progress in environmental-friendly polymer nanocomposite material from PLA: Synthesis, processing and applications. Vacuum 146:655–663. https://doi.org/10.1016/j.vacuum.2017.07.009
6. Kabir E, Kaur R, Lee J, Kim KH, Kwon EE (2020) Prospects of biopolymer technology as an alternative option for non-degradable plastics and sustainable management of plastic wastes. J Clean Prod 258:120536. https://doi.org/10.1016/j.jclepro.2020.120536
7. Kakadellis S, Harris ZM (2020) Don't scrap the waste: The need for broader system boundaries in bioplastic food packaging life-cycle assessment – A critical review. J Clean Prod 274:122831. https://doi.org/10.1016/j.jclepro.2020.122831
8. Nagarajan V, Mohanty AK, Misra M (2016) Perspective on polylactic acid (PLA) based sustainable materials for durable applications: Focus on Toughness and Heat Resistance. ACS Sustainable Chem Eng 4(6):2899–2916. https://doi.org/10.1021/acssuschemeng.6b00321
9. Riaz S, Rhee KY, Park SJ (2021) Polyhydroxyalkanoates (PHAs): Biopolymers for Biofuel and Biorefineries. Polymers 13(2):253. https://doi.org/10.3390/polym13020253
10. Riaz S, Raza ZA, Majeed MI, Jan T (2018) Synthesis of zinc sulfide nanoparticles and their incorporation into poly (hydroxybutyrate) matrix in the formation of a novel nanocomposite. Mater Res Express 5(5):055027. https://doi.org/10.1088/2053-1591/aac1f9
11. Raza ZA, Riaz S, Banat IM (2018) Polyhydroxyalkanoates: Properties and chemical modification approaches for their functionalization. Biotechnol Prog 34(1):29–41. https://doi.org/10.1002/btpr.2565
12. Charlon S, Follain N, Dargent E, Soulestin J, Sclavons M, Marais S (2016) Poly[(butylene succinate)-co-(butylene adipate)]-montmorillonite nanocomposites prepared by water-assisted extrusion: Role of the dispersion level and of the structure-microstructure on the enhanced barrier properties. J Phys Chem C 120(24):13234–13248. https://doi.org/10.1021/acs.jpcc.6b00339
13. Li J, Lai L, Wu L, Severtson SJ, Wang WJ (2018) Enhancement of water vapor barrier properties of biodegradable poly(butylene adipate-co-terephthalate) films with highly oriented organomontmorillonite. ACS Sustainable Chem Eng 6(5):6654–6662. https://doi.org/10.1021/acssuschemeng.8b00430
14. Inkinen S, Hakkarainen M, Albertsson AC, Södergård A (2011) From lactic acid to poly(lactic acid) (PLA): Characterization and analysis of PLA and Its precursors. Biomacromolecules 12(3):523–532. https://doi.org/10.1021/bm101302t
15. Zhang K, Nagarajan V, Misra M, Mohanty AK (2014) Supertoughened renewable PLA reactive multiphase blends system: Phase morphology and performance. ACS Appl Mater Interfaces 6(15):12436–12448. https://doi.org/10.1021/am502337u
16. Tyler B, Gullotti D, Mangraviti A, Utsuki T, Brem H (2016) Polylactic acid (PLA) controlled delivery carriers for biomedical applications. Adv Drug Deliv Rev 107:163–175. https://doi.org/10.1016/j.addr.2016.06.018
17. Hamad K, Kaseem M, Ayyoob M, Joo J, Deri F (2018) Polylactic acid blends: The future of green, light and tough. Prog Polym Sci 85:83–127. https://doi.org/10.1016/j.progpolymsci.2018.07.001
18. Lu H, Madbouly SA, Schrader JA, Srinivasan GG, McCabe KG, Grewell D, Kessler MR, Graves WR (2014) Biodegradation behavior of poly(lactic acid) (PLA)/distiller's dried grains with solubles (DDGS) composites. ACS Sustainable Chem Eng 2(12):2699–2706. https://doi.org/10.1021/sc500440q
19. Cesur S, Oktar FN, Ekren N, Kilic O, Alkaya DB, Seyhan SA, Ege ZR, Lin CC, Kuruca SE, Erdemir G, Gunduz O (2020) Preparation and characterization of electrospun polylactic acid/sodium alginate/orange oyster shell composite nanofiber for biomedical application. J Aust Ceram Soc 56:533–543. https://doi.org/10.1007/s41779-019-00363-1
20. Roth M, Jekle M, Becker T (2019) Opportunities for upcycling cereal byproducts with special focus on Distiller's grains. Trends Food Sci Technol 91:282–293. https://doi.org/10.1016/j.tifs.2019.07.041
21. DeRose K, Liu F, Davis RW, Simmons BA, Quinn JC (2019) Conversion of distiller's grains to renewable fuels and high value protein: Integrated techno-economic and life cycle assessment. Environ Sci Technol 53(17):10525–10533. https://doi.org/10.1021/acs.est.9b03273
22. Roth M, Meiringer M, Kollmannsberger H, Zarnkow M, Jekle M, Becker T (2014) Characterization of key aroma compounds in distiller's grains from wheat as a basis for utilization in the food industry. J Agric Food Chem 62(45):10873–10880. https://doi.org/10.1021/jf503281x
23. Villegas-Torres MF, Ward JM, Lye GJ (2015) The protein fraction from wheat-based dried distiller's grain with solubles (DDGS): extraction and valorization. N Biotechnol 32(6):606–611. https://doi.org/10.1016/j.nbt.2015.01.007
24. Tisserat B, Reifschneider L, O'Kuru RH, Finkenstadt VL (2013) Mechanical and thermal properties of high density polyethylene - dried distillers grains with solubles composites. Bioresources 8(1), 59–75. https://doi.org/10.15376/biores.8.1.59-75
25. Li C, Wu N, Zhang M, Wei C, Yan F, Wang Z (2018) Effects of E44 and KH560 modifiers on properties of distillers grains poly(butylene succinate) composites. Polym Compos 40(4):1499–1509. https://doi.org/10.1002/pc.24889
26. Hadiyanto H, Lestari SP, Abdullah A, Widayat W, Sutanto H (2016) The development of fly ash-supported CaO derived from mollusk shell of Anadara granosa and *Paphia undulata* as heterogeneous CaO catalyst in biodiesel synthesis. Int J Energy Environ Eng 7:297–305. https://doi.org/10.1007/s40095-016-0212-6
27. Kao CY, Huang YC, Chiu SY, Kuo KL, Hwang PA (2018) Bacteriostatic effect of a calcined waste clamshell-activated plastic film for food packaging. Materials 11(8):1370. https://doi.org/10.3390/ma11081370
28. Wu CS, Liao HT (2017) Polyester-based green composites for three-dimensional printing strips: Preparation, characterization and antibacterial properties. Polym Bull 74(6):2277–2295. https://doi.org/10.1007/s00289-016-1836-7
29. Wu CS, Wu DY, Wang SSA (2019) Antibacterial properties of biobased polyester composites achieved through modification with a thermally treated waste scallop shell. ACS Appl Bio Mater 2(5):2262–2270. https://doi.org/10.1021/acsabm.9b00205
30. Wu CS (2018) Solar energy tube processing of lemon residues for use as fillers in polyester-based green composites: characterization and biodegradability. Polym Bull 75(12):5745–5761. https://doi-org.ezproxy.lib.ntust.edu.tw/10.1007/s00289-018-2359-1
31. Wu CS, Liao HT, Cai YX (2017) Characterisation, biodegradability and application of palm fibre reinforced polyhydroxyalkanoate composites. Polym Degrad Stab 140:55–63. https://doi.org/10.1016/j.polymdegradstab.2017.04.016
32. Hsu YC, Wu CS, Liao HT, Cai YX (2015) Improvement of biocompatibility of Polyhydroxyalkanoate by filling with hyaluronic acid. J Mater Sci 50(23):7790–7799. https://doi.org/10.1007/s10853-015-9350-0
33. Wu CS, Shih WL, Liao HT, Chan WC, Tsou CH (2018) Fabrication, characterization, cytocompatibility, and biological activity of lemon fiber-filled polyester composites. Int J Polym Mater Polym Biomater 67(3):151–160. https://doi.org/10.1080/00914037.2017.1309542

34. Wu CS (2018) Interface design, cytocompatibility, and biological activity of astaxanthin powder-filled polycaprolactone composites. Int J Polym Mater Polym Biomater 67(9):151–160. https://doi.org/10.1080/00914037.2017.1354203
35. Wu CS (2016) Modulation, functionality, and cytocompatibility of three-dimensional printing materials made from chitosan-based polysaccharide composites. Mater Sci Eng C 69:27–36. https://doi.org/10.1016/j.msec.2016.06.062
36. Shih YF (2007) Mechanical and thermal properties of waste water bamboo husk fiber reinforced epoxy composites. Mater Sci Eng A 445–446:289–295. https://doi.org/10.1016/j.msea.2006.09.032
37. Wu CS, Liao HT (2017) Interface design and reinforced features of arrowroot (Maranta arundinacea) starch/polyester-basedmembranes:modulation, antioxidant activity, and cytocompatibility. Mater Sci Eng C 70:54–61. https://doi.org/10.1016/j.msec.2016.08.067
38. Wu CS, Tsou CH (2019) Fabrication, characterization, and application of biocomposites from poly(lactic acid) with renewable rice husk as reinforcement. J Polym Res 26(2):44. https://doi.org/10.1007/s10965-019-1710-z
39. Liu X, Zhang L, Sun W, Zhang M, Yu S (2017) One-step preparation of sulfonated carbon-based solid acid from distillers' grain for esterification. Res Chem Intermed 43:5917–5932. https://doi.org/10.1007/s11164-017-2971-y
40. Wu CS (2015) Renewable resource-based green composites of surface-treated spent coffee grounds and polylactide: Characterisation and biodegradability. Polym Degrad Stab 121:51–59. https://doi.org/10.1016/j.polymdegradstab.2015.08.011
41. Jiang N, Li Y, Li Y, Yu T, Li Y, Li D, Xu J, Wang C, Shi Y (2020) Effect of short jute fibers on the hydrolytic degradation behavior of poly(lactic acid). Polym Degrad Stab 178:109214. https://doi.org/10.1016/j.polymdegradstab.2020.109214
42. Ngaowthong C, Boruvk M, Behálek L, Lenfeld P, Švec M, Dangtungee R, Siengchin S, Rangappa SM, Parameswaranpillai J (2019) Recycling of sisal fiber reinforced polypropylene and polylactic acid composites: Thermo-mechanical properties, morphology, and water absorption behavior. Waste Manag 97:71–81. https://doi.org/10.1016/j.wasman.2019.07.038
43. Guido LF, Moreira MM (2017) Techniques for extraction of brewer's spent grain polyphenols: a review. Food Bioproc Tech 10:1192–1209. https://doi.org/10.1007/s11947-017-1913-4
44. Wang X, Wang S, Huang S, Zhang L, Ge Z, Sun L, Zong W (2019) Purification of polyphenols from distiller's grains by macroporous resin and analysis of the polyphenolic components. Molecules 24:1284. https://doi.org/10.3390/molecules24071284
45. Tsou CH, Wu CS, Hung W-S, De Guzman MR, Gao C, Wang R-Y, Chen J, Wan N, Peng YJ, Suen MC (2019) Rendering polypropylene biocomposites antibacterial through modification with oyster shell powder. Polymer 160:265–271. https://doi.org/10.1016/j.polymer.2018.11.048